applied sciences

MDPI

Article

Identification of Common Liver Metabolites of the Natural Bioactive Compound Erinacine A, Purified from *Hericium erinaceus* Mycelium

Yu-Hsuan Kuo [1], Ting-Wei Lin [1], Jing-Yi Lin [1], Yu-Wen Chen [1], Tsung-Ju Li [1,*] and Chin-Chu Chen [1,2,3,4,*]

[1] Biotech Research Institute, Grape King Bio, Taoyuan 32542, Taiwan; yuhsuan.kuo@grapeking.com.tw (Y.-H.K.); tingwei.lin@grapeking.com.tw (T.-W.L.); jingyi.lin@grapeking.com.tw (J.-Y.L.); annie.chen@grapeking.com.tw (Y.-W.C.)
[2] Department of Food Science, Nutrition, and Nutraceutical Biotechnology, Shih Chien University, Taipei City 11031, Taiwan
[3] Bioscience Technology, Chung Yuan Christian University, Taoyuan 32023, Taiwan
[4] Institute of Food Science and Technology, National Taiwan University, Taipei City 10617, Taiwan
* Correspondence: tsungju.li@grapeking.com.tw (T.-J.L.); drccchen@g2.usc.edu.tw (C.-C.C.)

Abstract: Metabolite identification, in the early stage, for compound discovery is necessary to assess the knowledge for the pharmaceutical improvement of drug safety and efficacy. Even if the drug has been released into the market, identification and continuous evaluation of the metabolites are required to avoid the risk of post-marketing withdrawal. *Hericium erinaceus* (HE), a medicinal mushroom, has broadly documented nutraceutical benefits, including anti-oxidant, anti-tumor, anti-aging, hypolipidemic, and gastric mucosal protection effects. Recently, erinacine A has been reported as the main natural bioactive compound in the mycelium of HE for functional food development. In neurological studies, the consumption of enrinacine A enriched HE mycelium demonstrates its significant nutraceutical effects in Alzheimer's disease, Parkinson's disease, and ischemic stroke. For the first time, we explored the metabolic process of erinacine A molecule and identified its metabolites from the rat and human liver S9 fraction. Using a liquid chromatography/triple quadrupole mass spectrometer for quantitative analysis, we observed that 75.44% of erinacine A was metabolized within 60 min in rat, and 32.34% of erinacine A was metabolized within 120 min in human S9. Using an ultra-performance liquid chromatography/quadrupole time-of-flight mass spectrometry (UPLC-QTOF/MS) to identify the metabolites of erinacine A, five common metabolites were identified, and their possible structures were evaluated. Understanding the metabolic process of erinacine A and establishing its metabolite profile database will help promote the nutraceutical application and discovery of related biomarkers in the future.

Keywords: erinacine A; metabolites; *Hericium erinaceus* mycelium; mass spectrometry

Citation: Kuo, Y.-H.; Lin, T.-W.; Lin, J.-Y.; Chen, Y.-W.; Li, T.-J.; Chen, C.-C. Identification of Common Liver Metabolites of the Natural Bioactive Compound Erinacine A, Purified from *Hericium erinaceus* Mycelium. *Appl. Sci.* **2022**, *12*, 1201. https://doi.org/10.3390/app12031201

Academic Editors: Hari Prasad Devkota and Anna Lante

Received: 3 December 2021
Accepted: 20 January 2022
Published: 24 January 2022

1. Introduction

The liver is considered the second-largest organ in the body [1]. After food and drugs enter the gastrointestinal tract through the oral cavity, the gastrointestinal pili will absorb digested nutrients and drugs. The portal vein system will receive the blood flow collected by the gastrointestinal tract and enter the liver for preliminary treatment of the nutrients, metabolites, and drug molecules [2,3]. Metabolism is often divided into two phases of a biochemical reaction. Phase I involves oxidation, reduction, or hydrolysis by enzymes in the body. Phase II engages in the conjugation with small endogenous substances, turning them into highly soluble metabolites, enabling metabolites to be exported into the sinusoidal circulation for renal clearance, or into bile, which is then excreted from the body through urine or feces [4–6]. Metabolite identification in the early stage of drug discovery is necessary to assess the knowledge for improving pharmaceutical property, safety, and

efficacy of the bioactive molecule. Identification of metabolites and reactive intermediates suggest the need for structural modifications in investigational compounds to avoid subsequent toxic consequences. Even if the drug has been on the market, identification of the metabolites and evaluation is required to avoid the risk of their post-marketing withdrawal [7,8]. Therefore, in vitro, S9 fractions analysis provides several advantages compared to time-consuming in vivo studies: (1) they are amenable to high throughput screening and automation; (2) using S9 fraction allows for the testing of large quantities of compounds for drug discovery in a short period; (3) helps to reduced animal usage [9].

Hericium erinaceus (HE) is an edible mushroom that inhabits mountainous areas of the northeast territories in Asia [10], Europe, and North America [11]. HE belongs to Basidiomycota (Phylum), Agaricomycetes (Class), Russulales (Order), Hericiaceae (Family), and Hericium (Genus). HE has been documented to display a wide range of beneficial properties, including anti-oxidant, anti-tumor, anti-aging, hypolipidemic, and gastric mucosal protection effects [12–14]. In 1994, Kawagishi et al. discovered that the diterpenoid erinacine A, B, and C, in the mycelium of HE, could promote the production of stellate cell lines in the rat brain and the stimulation of nerve growth factor (NGF) synthesis [15]. Erinacine A can confer neuroprotective effects and attenuates oxidative stress against stroke [16], Alzheimer's disease [17], Parkinson's disease [18], ischemic stroke, and depression in vivo [19,20]. Moreover, erinacine A can pass through the blood-brain barrier of rats to support the development of HE mycelia as a functional food for neuro health improvement [21]. This edible mushroom mycelium has become a hot issue with researchers attempting to understand its important role in the central and peripheral nerves' development, differentiation, growth, and regeneration [22]. Recent studies have also showed that erinacine A enriched HE has potential benefits in treatment of Alzheimer's and Parkinson's disease [23–25]. However, no study has discussed erinacine A's possible metabolic biomarkers that may contribute to this nutraceutical effects.

In this study, erinacine A compound was purified from the erinacine A enriched HE mycelium and was metabolized using two different liver S9 fractions: rat and human. Using liquid chromatography/triple quadrupole mass spectrometer (HPLC-QQQ/MS) for quantitative analysis of erinacine A, and ultra-performance liquid chromatography/quadrupole time-of-flight mass spectrometry (UPLC-QTOF/MS) to identify the metabolites of erinacine A at each time point. We aim to understand the metabolic rate of erinacine A and establish its metabolite profile database to help promote the application of nutraceutical supplements and the research of potential medication in the future.

2. Materials and Methods

2.1. Materials and Reagents

The HE strain (BCRC 35669) was obtained from the Bioresources Collection and Research Center in Food Industry Research and Development Institute, Hsinchu, Taiwan. The strain was first grown in an ager slant before being transferred to a potato dextrose ager plate at 26 °C for 15 days. On day 15, the HE cultures were transferred to 1.3 L of liquid medium (in 2 L flasks). The liquid culture was shaken at 120 rev/min 25 °C for 5 days. Next, they were scaled up in 500 L, 20-ton fermenters for 5 days and 12 days, respectively. The culture medium is adjusted at pH 4.5 and contains 4.5% glucose, 0.5% soybean powder, 0.25% yeast extract, 0.25% peptone, and 0.05% MgSO4. Finally, the HE mycelia were harvested at the end of the 20-ton fermentation process. These raw materials were lyophilized, grounded in powder, and stored in a desiccator. Erinacine A was then extracted from the HE and quantified according to previous studies [26]. Methanol (LC-MS grade) was obtained from Merck (Darmstadt, Germany); acetonitrile (LC-MS grade), formic acid (FA, LC-MS grade, 98% purity), and ammonium acetate (98% purity) were obtained from Honeywell (Honeywell Burdick and Jackson, Muskegon, MI, USA). The rat liver S9 fraction was obtained from Moltox (Boone, NC, USA). The human liver S9 fraction was obtained from Thermo Fisher Scientific (Rockford, IL, USA).

2.2. Rat and Human Liver S9 Fraction

One milliliter of S9 stock solution was prepared in Regensys buffer, containing 1 mg/mL concentration of S9 and 0.5 M Potassium phosphate with NADPH, according to the kit recommendation. The prepared solution was kept at 4 °C until the erinacine A compound (10 μM) was added, followed by activation in a 37 °C water bath. When the metabolic time had reached its time points, 150 μL of the solution was withdrawn from the stock solution and quenched by adding two volumes of ice-cold ACN. The stopped solution is then transferred to QTOF for further metabolite analysis.

2.3. Instrumentation and Conditions

HPLC-QQQ/MS analysis was performed on an Agilent 1100 series HPLC system (Agilent, Palo Alto, CA, USA) coupled with an API 3000 triple quadrupole mass spectrometer (Applied Biosystems, Warrington, UK), with a Turbo-assisted ion spray (ESI) ionization source in a positive ionization mode. Chromatographic separation was conducted on an Agilent Eclipse XDB-C18 (4.6 mm × 100 mm × 3.5 μm). The column temperature was maintained at 22 °C. The mobile phase consisted of water containing 0.1% formic acid (A) and methanol (B). Gradient elution was used, starting with 70% B, increasing to 100% B within 5 min, holding for 3 min with 90% B, decreasing B to 70% within 0.1 min, and re-equilibration at 70% B for 2.9 min. A flow rate of 350 μL/min was applied, and a volume of 10 μL was injected.

Detection was performed with an ionizing voltage of +4500 V. Ion source temperature was set at 350 °C, with ultrahigh-purity nitrogen as curtain gas (7 psi). Nebulizer gas was 8 psi. Other mass-dependent parameters, such as declustering potential (DP), entrance potential (EP), focusing potential (FP), and collision energy (CE) for each compound, were determined in positive mode using standard solutions. Multiple reaction monitoring (MRM) was carried out using nitrogen as collision gas (2 psi) and with a dwell time of 200 ms for each transition. Erinacine A was detected by monitoring the transitions *m/z* 443.200 → 301.200, 283.200. The data were analyzed using Analyst 1.4.2 software (Applied Biosystems, Concord, ON, Canada) and Graphpad (Prism 8.0.0.).

UPLC-QTOF/MS analysis was performed on an Agilent 1290 Infinity II UPLC system (Agilent, Palo Alto, CA, USA), coupled with an Agilent 6546 quadrupole time-of-flight mass spectrometry (Agilent, Palo Alto, CA, USA). Chromatographic separation was conducted on a Phenomenex Kinetex® C18 LC Column (3 mm × 100 mm × 1.7 μm). The column temperature was maintained at 40 °C. The mobile phase A consisted of water containing 0.1% (*v*/*v*) formic acid in positive mode, 0.1% (*v*/*v*) formic acid, and 10 mM CH_3COONH_4 in negative mode. The mobile phase B was acetonitrile. Gradient elution was used, starting with 5% B and holding for 0.5 min, increasing to 50% B within 5.5 min, increasing to 100% B within 10 min, and holding for 6 min. A flow rate of 400 μL/min was applied, and a volume of 2 μL was injected.

Agilent 6546 quadrupole time-of-flight mass spectrometry was equipped with an electrospray ionization (ESI) source. The data acquisition was under the control of Mass Hunter workstation software. The typical operating source conditions in positive and negative ion ESI mode were optimized as follows: ion spray voltage (ESI^+/ESI^-) were 4000 V/3000 V; the gas temperature was 320 °C; drying gas flow rate was 8 L/min; nebulizer pressure was 45 psi; sheath gas temperature was 350 °C; sheath gas flow rate was 12 L/min; the collision energy was 10, 20, 40, and 60 V. Metabolites were identified using Agilent MassHunter Biotransformation software (version B.04.00) (Santa Clara, CA, USA). Chromatograms and mass spectra of the parent and identified metabolites were extracted using Agilent MassHunter Qualitative Analysis software (version B.05.00) (Santa Clara, CA, USA).

3. Results and Discussion

3.1. Quantification of Erinacine A in Rat and Human Liver S9 Analysis

Erinacine A was examined using rat and human liver S9 fraction and quantified by HPLC-QQQ/MS at different time points. The remaining verses time profile of erinacine

A, in rat and human liver S9 fraction treatment, are shown in Figure 1. Using the 'well-stirred model' and formula calculation [27], the predicted value is shown in Table 1. Rat liver S9 metabolized ~75.4% of erinacine A within 60 min. Human liver S9 metabolized ~49.8% of erinacine A within 120 min. In the presence of NADPH, erinacine A was metabolized more slowly, with a $t_{1/2}$ = 114.92 min in human. E_H is the fraction of drug being filtered by the liver in one pass, in which the drug is irreversibly removed (extracted). We found that the E_H of rat was higher than that of human. This result is reasonable, judging from $t_{1/2}$ values, because rat liver has been reported to metabolize faster than human liver [28]. Compared with other compound reports using rat liver S9, GKB202 of the *Antrodia cinnamomea* mycelium ($t_{1/2}$ = 3.68 min) was metabolized more rapidly than erinacine A [29].

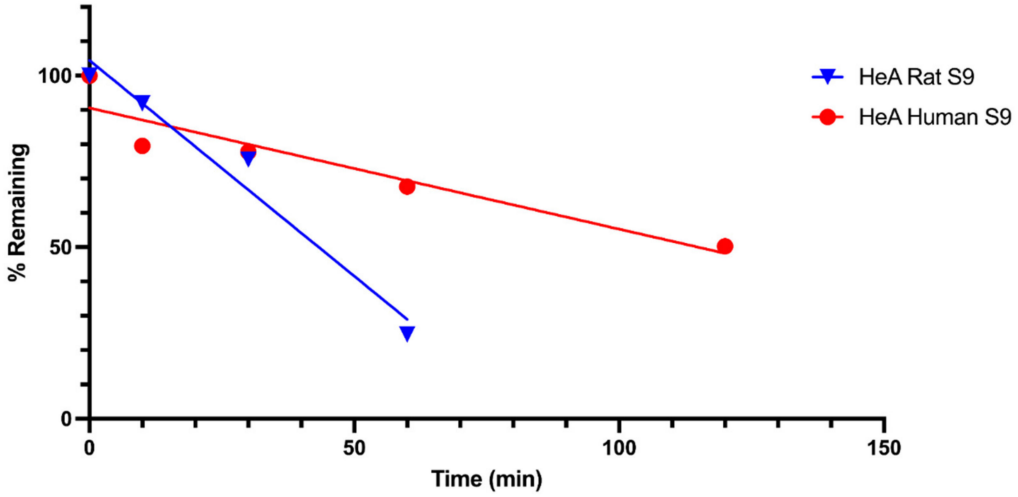

Figure 1. Erinacine A remaining versus time profile in rat and human liver S9. Data is presented in mean values of triplicate measurements.

Table 1. Hepatic metabolic stability of erinacine A in rats and humans.

Species	$t_{1/2}$ (min)	CL_{int} (mL/min/kg)	CL_H (mL/min/kg)	E_H
Rat	43.32	87.02	3.7	0.61
Human	114.92	18.92	9.72	0.49

$t_{1/2}$: half-life, CL_{int}: hepatic intrinsic clearance, CL_H: hepatic clearance, E_H: hepatic extraction ratio.

The previous report showed that there was no-observed-adverse-effect of 3 g/kg body weight/day erinacine A-enriched HE in 28-day oral feeding in Sprague–Dawley rats. The current study dosage input for liver cells metabolism gives a reasonable correlation, with a previous in vivo study, of erinacine A compound pharmacokinetics (PK) [30,31]. In one recent in vivo report, the Tsai et al. group detected erinacine A in rat plasma after oral administration of HE mycelia (50 mg/kg) at 60 min [32]. This can correlate with the current in vitro finding, in which we demonstrated, theoretically, that there is still ~24.6% remaining of the compound after rat liver S9 metabolism. In addition, approximately half of unmetabolized erinacine A were found in the remaining human liver S9, demonstrating that complete compound structures could enter the bloodstream, which contributes to its effectiveness in neuroprotection. Whether or not the common metabolites provide, the biological function is still under investigation and will be reported in a separate study.

3.2. In Vitro Metabolite Identification in Rat and Human

Ultra-performance liquid chromatography/quadrupole time-of-flight mass spectrometry (UPLC-QTOF/MS) was used to identify the metabolites in the positive and negative modes. A comparison of erinacine A metabolites, in this study, with rat and human liver S9 metabolites is shown in Table 2. Twenty-four metabolites were found after erinacine

A incubation and were assigned as M1-M24 (Table S1). Five common metabolites were detected after incubation with rat and human liver S9. The mass errors were all ≤5 ppm. The top three abundant metabolites, based on peak area, were Gluthation conjugation + Demethylation (M6), Demethylation (M2), and Demethylation + Hydrogenation (M3). Alcohols Dehydration (M1), Demethylation (M2), Demethylation + Hydrogenation (M3), 2 × Hydroxylation (M4), Demethylation, and two Hydroxylations (M5) metabolites were both identified in rat and human liver S9. The proposed metabolic pathway and possible metabolites of erinacine A are shown in Figure 2.

Table 2. Common liver metabolites of erinacine A, detected in rat and human liver S9, with an UPLC-QTOF/MS.

ID	Metabolic Reaction	Formula	RT	Exact Mass	Mass Error (ppm)	Accurate Mass	Fragment	Polarity	Rat	Human
Parent	Erinacine A	$C_{25}H_{36}O_6$	8.782	432.2515	0.73	432.2512	119.0859, 199.1492, 240.1464, 283.2055, 301.2162 *	Positive	v	v
M1	Alcohols Dehydration	$C_{25}H_{34}O_5$	8.799	414.2399	−1.63	414.2406	69.0327, 105.0709, 119.0856 *, 135.0817, 181.1249, 235.1701, 283.2036	Positive	v	v
M2	Demethylation	$C_{24}H_{34}O_6$	4.916	418.2354	−0.25	418.2355	97.0289, 123.0551 *, 179.0486, 231.0436, 368.9803	Positive	v	v
M3	Demethylation + Hydrogenation	$C_{24}H_{36}O_6$	13.28	420.2488	−4.72	420.2512	55.0539, 77.0054 *, 95.0854, 147.1172, 277.2183, 353.2141	Positive	v	v
M4	2 × Hydroxylation	$C_{25}H_{36}O_8$	4.071	464.2405	−1.41	464.241	89.0597 *, 133.0860, 177.1115, 297.1842	Positive	v	v
M5	Demethylation and two Hydroxylations	$C_{24}H_{34}O_8$	8.777	450.2265	2.44	450.2254	59.0601 *, 101.0705, 178.1225, 321.1516	Positive	v	v

* Rat liver S9: M1 was detected at 10, 30 min, M2 and M3 were detected at 60 min, M4 and M5 were detected at 10, 30, 60 min. Human liver S9: M1, M2, M3, and M4 were detected at 10, 30, 60, 120 min, M5 was detected at 120 min.

The parent compound of the erinacine A formula was $C_{25}H_{36}O_6$. The MS spectrum of erinacine A was found at $[M + H]^+$ = 433.2573 and $[M + Na]^+$ = 455.2405 (Figure 3A). The MS/MS spectrum by the collision energy of 10 V is shown Figure 3B that correspond to the cleavage of the C-O ether bond ($[C_{20}H_{29}O_2]^+$ = 301.2162 and $[C_{20}H_{27}O]^+$ = 283.2052) (Figure 3C) [15,32]. The Alcohols Dehydration metabolites (M1) formula was $C_{25}H_{34}O_5$, with erinacine A losing an H_2O [33,34]. The MS spectrum of M1 was found at $[M + H]^+$ = 415.2472 and $[M + Na]^+$ = 437.2255. At a collision energy of 10V, the main product ions were *m/z* 283.2036, 215.1701, 181.1249, 135.0817, 119.0856, 105.0709, and 69.0327 (Figure 4A). Two product ions were analogous to those of erinacine A ions (*m/z* 283.2036 and *m/z* 119.0856), and the product ion of *m/z* 301.2162 disappeared. Dehydrated M1 could be used to indicate water loss in pentose fragments [35]. The Demethylation metabolites (M2) formula was $C_{24}H_{34}O_6$, with erinacine A losing a methylene (-CH_2) [36]. At a collision energy of 40 V, the MS spectrum of M2 was found at $[M + H]^+$ = 419.2407. The main product

ions were *m/z* 312.0488, 269.9469, 231.0432, 123.0552, and 179.0486 (Figure 4B). The product ion at *m/z* 269.9469, 179.0486 corresponded to cleavage of the methylene (-CH_3) and plus H^+. The Demethylation + Hydrogenation metabolites (M3) formula was $C_{24}H_{36}O_6$ with M2 reduction in alkene (+H_2) [37–39]. The MS spectrum of M3 was found at $[M + H]^+$ = 421.2569 and $[M + Na]^+$ = 443.2355. At a collision energy of 40 V, the main product ions were *m/z* 353.2141, 277.2183, 147.1172, and 77.0054 (Figure 4C). The product ion at *m/z* 353.2141, 277.2183 were corresponding to Hydrogenation. The 2 × Hydroxylation metabolites (M4) formula was $C_{25}H_{36}O_8$ with erinacine A Hydroxylation of isopropyl side chain and cyclopentene [40–42]. The MS spectrum of M4 was found at $[M + H]^+$ = 465.2461 and $[M + Na]^+$ = 487.2315. At collision energy of 20V, the main product ions were *m/z* 297.1842, 255.1389, 177.1115, 133.0860, and 89.0597 (Figure 4D). The product ion at *m/z* 297.1842, and 89.0598 were corresponding to Hydroxylation. The Demethylation and two Hydroxylation metabolites (M5) formula was $C_{24}H_{34}O_8$ with M11 losing a methylene (-CH_2). The MS spectrum of M5 was found at $[M + H]^+$ = 451.2413 and $[M + Na]^+$ = 473.2158. At collision energy of 40 V, the main product ions were *m/z* 321.1516, 178.1225, 101.0705, and 59.0601 (Figure 4E). The product ion at *m/z* 321.1516 corresponded to M4 cleavage of the methylene (-CH_3) and plus H^+.

There have been 70 different secondary metabolites isolated from either HE sporophore or mycelium. These metabolites are identified as polysaccharides, polyketides, phenols, terpenoids, and bioactive molecules [43–45]. We speculated that these common metabolites, which we analyzed, might also be the precursors or intermediate products of the mycelium secondary metabolites mentioned before. Nevertheless, it has been reported that M1, M2, M3, M4, and M5 may represent key intermediates between erinacine A and secondary metabolites for rat and human studies. Due to the increasing use of HE mycelium as a functional supplement, identifying these metabolites will also reveal useful biomarkers. Taking cholesterol as an example, the precursors or intermediate products of various substances, produced by the liver enzymes process, were metabolized to oxysterol, which is now understood as a potent metabolite in sterol metabolism and synthesis regulation [46].

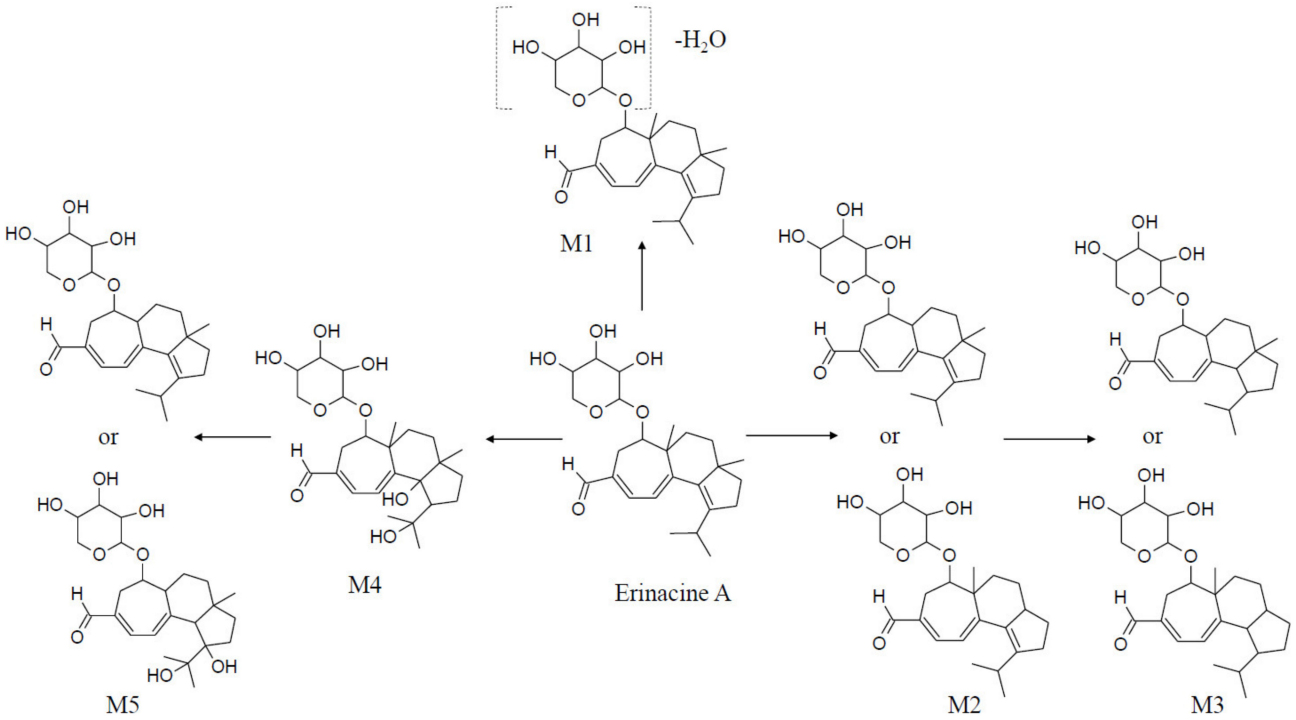

Figure 2. Proposed metabolic pathway of erinacine A.

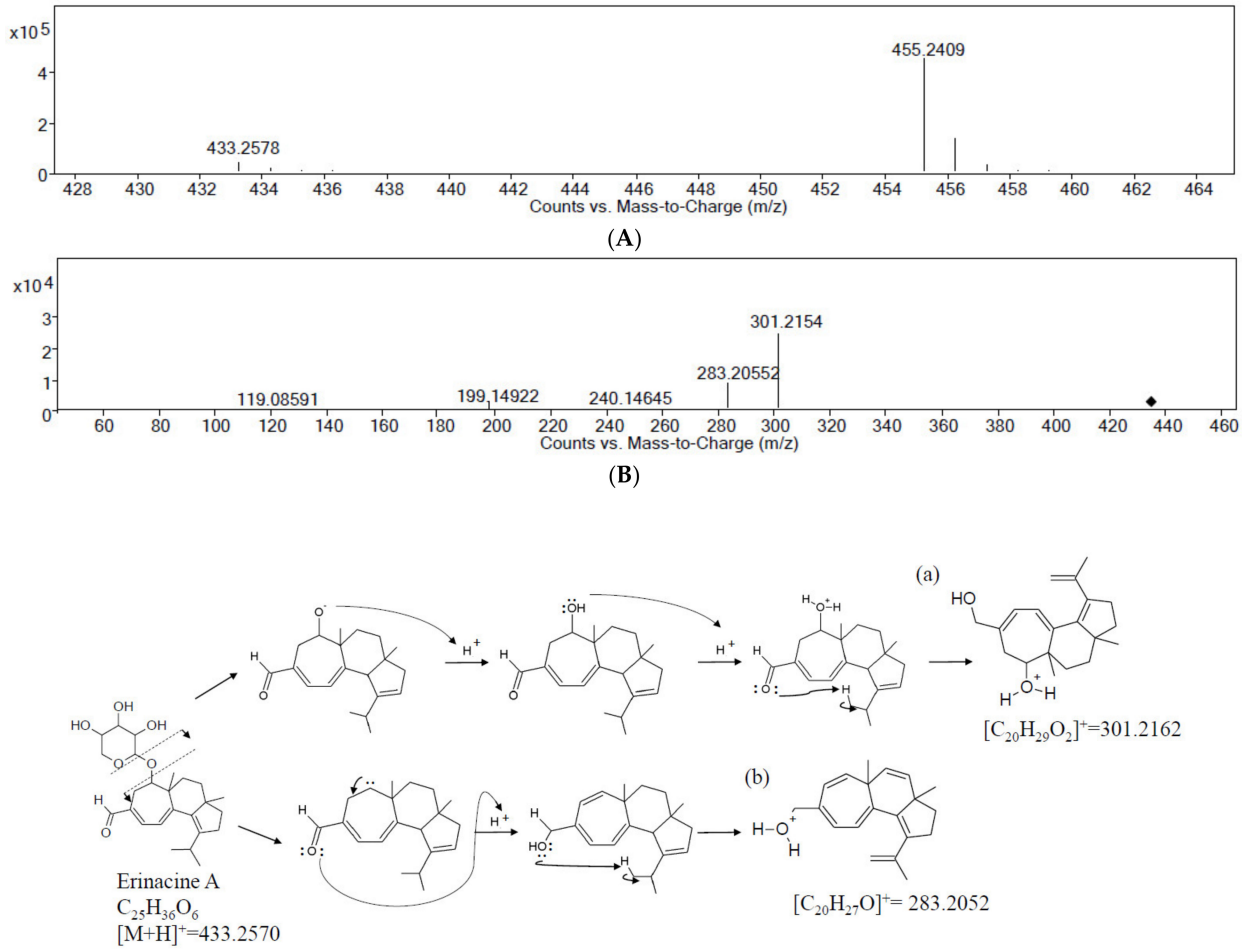

Figure 3. (**A**) MS spectrum of erinacine A with an ultra-high performance liquid chromatography tandem quadrupole time-of-flight mass spectrometry. (**B**) MS/MS spectrum of erinacine A with an ultra-high performance liquid chromatography tandem quadrupole time-of-flight mass spectrometry. (**C**) The proposed structures of product ions, produced by erinacine A, at a collision energy of 10 V. (a) $[C_{20}H_{29}O_2]^+$ = 301.2162, (b) $[C_{20}H_{27}O]^+$ = 283.2052. ♦: Parent ion.

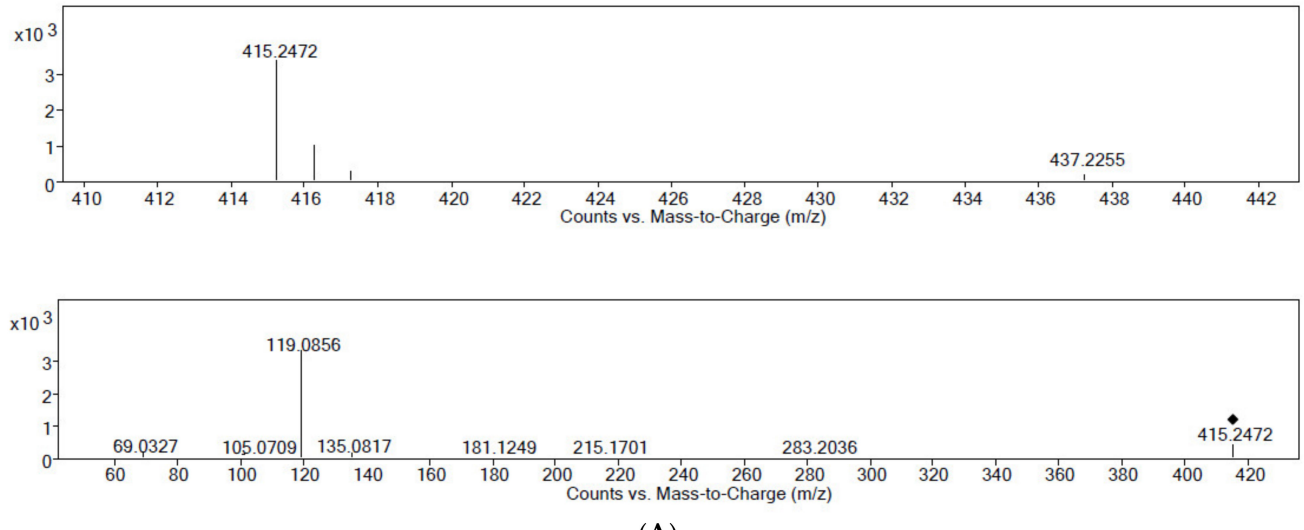

Figure 4. *Cont*.

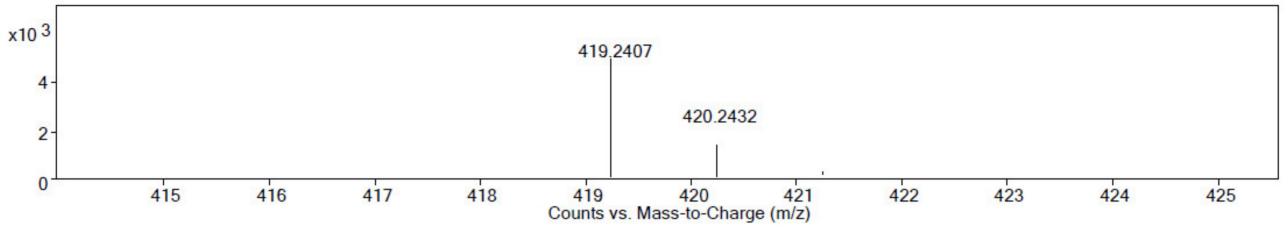

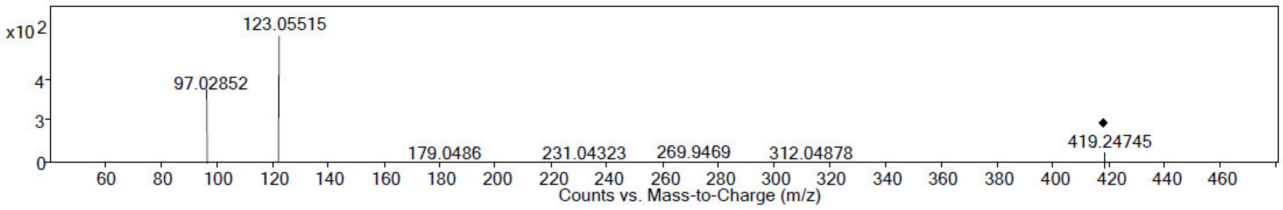

(**B**)

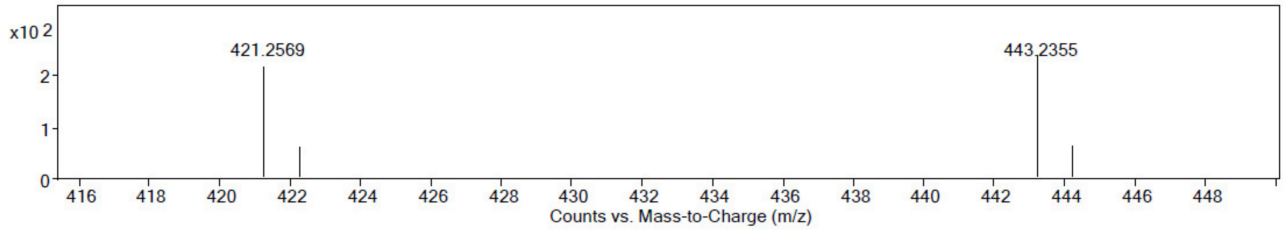

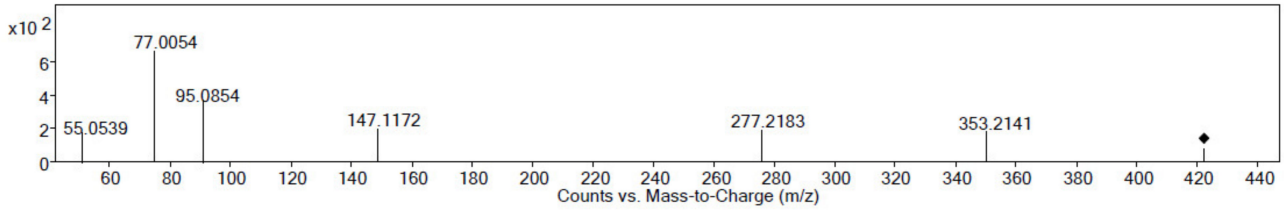

(**C**)

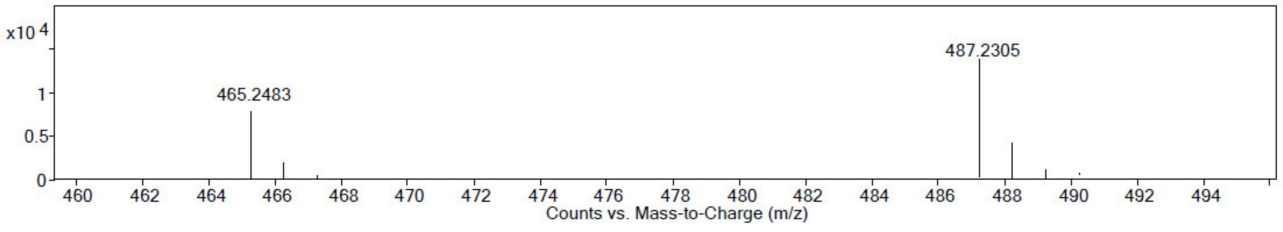

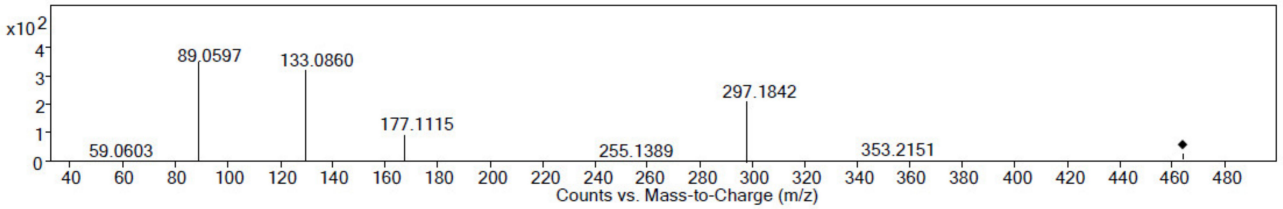

(**D**)

Figure 4. *Cont*.

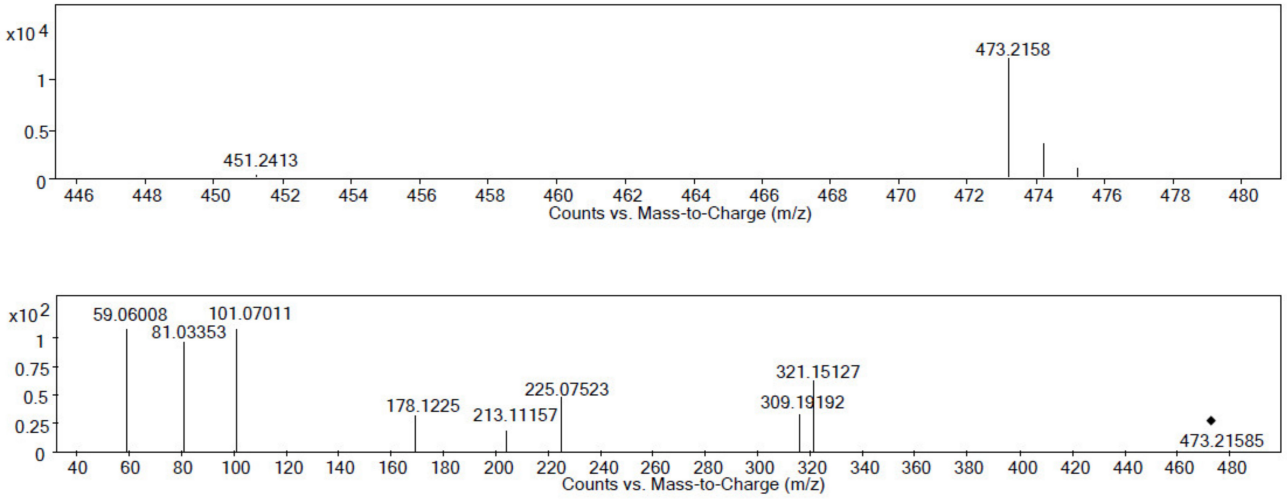

(**E**)

Figure 4. MS and MSMS spectrum of (**A**) Alcohols Dehydration (M1), (**B**) Demethylation metabolites (M2), (**C**) Demethylation + Hydrogenation metabolites (M3), (**D**) 2 × Hydroxylation metabolites (M4), (**E**) Demethylation and two Hydroxylations (M5) metabolite using an ultra-high performance liquid chromatography tandem quadrupole time-of-flight mass spectrometry. ♦: Parent ion.

M2 and M3 were detected at 60 min for rat liver S9, whereas for human liver S9, M2 and M3 were detected at 10, 30, 60, and 120 min. We conjectured that M3 might be produced by two distinct metabolic pathways; one from erinacine A to M3, and the other was derived from M1. In contrast, M4 and M5 were detected at 10, 30, and 60 min rat liver S9. In human liver S9, M4 was detected at 10, 30, 60, and 120 min. M5 was detected at 120 min. The time of appearance can explain that M5 metabolic pathway may be derived from M4.

This study provides additional information for the HE mycelium clinical studies missing information, which is the metabolic action from the bioactive compound. In a recent randomized, double-blind placebo-controlled study, three 350 mg/g HE mycelia (containing 5 mg/g erinacine A) capsules intervention, for 49 weeks, demonstrated higher Cognitive Abilities Screening Instrument, Mini-Mental State Examination, and Instrumental Activities of Daily Living scores and achieved a better contrast sensitivity, in patients with age > 50 years old and diagnosis of probable Alzheimer's Disease, when compared to the placebo group [19]. By understanding erinacine A metabolites profile, we can interpret that erinacine A enriched HE mycelia improved neurocognitive disorder, which might be contributed mostly from the unmetabolized compound. As for erinacine A, metabolites are well-tolerated and might be important in achieving neuro-nutritional benefits, which will be investigated in future studies.

4. Conclusions

This is the first study to establish the mass spectrometry analysis of metabolic stability and identify of five common metabolites of erinacine A found in rat and human liver S9 fractions. The results from this study will help to understand the characteristics, safety, and efficacy of this unique bioactive compound. Our results indicate that erinacine A's clinical benefits may arise from the compound and its metabolites. In the future, we will analyze metabolites from blood, organs, and tissues to establish a complete metabolism database. Such work is expected to help functional research food, nutraceutical supplements, and precision medicine.

Supplementary Materials: The following are available online at https://www.mdpi.com/article/10.3390/app12031201/s1, Table S1: Identify of erinacine A metabolites in rat and human liver S9 with an UPLC-QTOF/MS.

Author Contributions: Data interpretation, Y.-H.K., T.-W.L., J.-Y.L., Y.-W.C. and T.-J.L.; methodology; Y.-H.K., T.-W.L. and T.-J.L.; investigation conducted by T.-J.L. and C.-C.C.; raw materials provided by: Y.-H.K., T.-W.L., J.-Y.L., Y.-W.C., T.-J.L. and C.-C.C.; visualization: Y.-H.K.; original draft preparation was done by Y.-H.K., T.-W.L., T.-J.L. and C.-C.C.; writing—review and editing, Y.-H.K., T.-J.L. and C.-C.C. All authors have read and agreed to the published version of the manuscript.

Funding: This research received no external funding.

Data Availability Statement: The raw materials and compounds presented in this study are available from the corresponding author upon request.

Conflicts of Interest: The authors declare no conflict of interest.

Sample Availability: Samples of the compounds are available from the authors.

References

1. Mitra, V.; Metcalf, J. Functional anatomy and blood supply of the liver. *Anaesth. Intensive Care Med.* **2009**, *10*, 332–333. [CrossRef]
2. Alamri, Z.Z. The role of liver in metabolism: An updated review with physiological emphasis. *Int. J. Basic Clin. Pharmacol.* **2018**, *7*, 2271. [CrossRef]
3. Russell-Jones, G. The potential use of receptor-mediated endocytosis for oral drug delivery. *Adv. Drug Deliv. Rev.* **1996**, *20*, 83–97. [CrossRef]
4. Shugarts, S.; Benet, L.Z. The role of transporters in the pharmacokinetics of orally administered drugs. *Pharm. Res.* **2009**, *26*, 2039–2054. [CrossRef]
5. Richardson, S.J.; April, B.; Kulkarni, A.A.; Moghaddam, M.F. Efficiency in Drug Discovery: Liver S9 Fraction Assay as a Screen for Metabolic Stability. *Drug Metab. Lett.* **2016**, *10*, 83–90. [CrossRef]
6. Corsini, A.; Bortolini, M. Drug-Induced Liver Injury: The Role of Drug Metabolism and Transport. *J. Clin. Pharmacol.* **2013**, *53*, 463–474. [CrossRef] [PubMed]
7. Lam, W.W.; Chen, J.; Xu, R.F.; Silva, J.; Lim, H.-K. Metabolite Identification in Drug Discovery. In *Optimization in Drug Discovery. Methods in Pharmacology and Toxicology*; Caldwell, G., Yan, Z., Eds.; Humana Press: Totowa, NJ, USA, 2014; pp. 445–459.
8. Prasad, B.; Garg, A.; Takwani, H.; Singh, S. Metabolite identification by liquid chromatography-mass spectrometry. *TrAC Trends Anal. Chem.* **2011**, *30*, 360–387. [CrossRef]
9. Zhang, D.; Luo, G.; Ding, X.; Lu, C. Preclinical experimental models of drug metabolism and disposition in drug discovery and development. *Acta Pharm. Sin. B* **2012**, *2*, 549–561. [CrossRef]
10. Wang, M.; Gao, Y.; Xu, D.; Konishi, T.; Gao, Q. *Hericium erinaceus* (Yamabushitake): A unique resource for developing functional foods and medicines. *Food Funct.* **2014**, *5*, 3055–3064. [CrossRef]
11. Hu, T.; Hui, G.; Li, H.; Guo, Y. Selenium biofortification in *Hericium erinaceus* (Lion's Mane mushroom) and its in vitro bioaccessibility. *Food Chem.* **2020**, *331*, 127287. [CrossRef]
12. Kim, K.H.; Noh, H.J.; Choi, S.U.; Lee, K.R. Isohericenone, a new cytotoxic isoindolinone alkaloid from Hericium erinaceum. *J. Antibiot.* **2012**, *65*, 575–577. [CrossRef]
13. Khan, M.A.; Tania, M.; Liu, R.; Rahman, M.M. *Hericium erinaceus*: An edible mushroom with medicinal values. *J. Complementary Integr. Med.* **2013**, *10*, 253–258. [CrossRef]
14. He, X.; Wang, X.; Fang, J.; Chang, Y.; Ning, N.; Guo, H.; Huang, L.; Huang, X.; Zhao, Z. Structures, biological activities, and industrial applications of the polysaccharides from *Hericium erinaceus* (Lion's Mane) mushroom: A review. *Int. J. Biol. Macromol.* **2017**, *97*, 228–237. [CrossRef]
15. Kawagishi, H.; Shimada, A.; Shirai, R.; Okamoto, K.; Ojima, F.; Sakamoto, H.; Ishiguro, Y.; Furukawa, S. Erinacines A, B and C strong stimulators of nerve growth factor (NGF)-synthesis from the mycelia of Hericium erinaceum. *Tetrahedron Lett.* **1994**, *35*, 1569–1572. [CrossRef]
16. Lee, K.F.; Chen, J.H.; Teng, C.C.; Shen, C.H.; Hsieh, M.C.; Lu, C.C.; Lee, K.C.; Lee, L.Y.; Chen, W.P.; Chen, C.C.; et al. Protective Effects of *Hericium erinaceus* Mycelium and Its Isolated Erinacine A against Ischemia-Injury-Induced Neuronal Cell Death via the Inhibition of iNOS/p38 MAPK and Nitrotyrosine. *Int. J. Mol. Sci.* **2014**, *15*, 15073–15089. [CrossRef]
17. Tzeng, T.T.; Chen, C.C.; Chen, C.C.; Tsay, H.J.; Lee, L.Y.; Chen, W.P.; Shen, C.C.; Shiao, Y.J. The Cyanthin Diterpenoid and Sesterterpene Constituents of *Hericium erinaceus* Mycelium Ameliorate Alzheimer's Disease-Related Pathologies in APP/PS1 Transgenic Mice. *Int. J. Mol. Sci.* **2018**, *19*, 598. [CrossRef]

18. Lee, L.-Y.; Chou, W.; Chen, W.-P.; Wang, M.-F.; Chen, Y.-J.; Chen, C.-C.; Tung, K.-C. Erinacine A-Enriched *Hericium erinaceus* Mycelium Delays Progression of Age-Related Cognitive Decline in Senescence Accelerated Mouse Prone 8 (SAMP8) Mice. *Nutrients* **2021**, *13*, 3659. [CrossRef]
19. Li, I.; Chang, H.-H.; Lin, C.-H.; Chen, W.-P.; Lu, T.-H.; Lee, L.-Y.; Chen, Y.-W.; Chen, Y.-P.; Chen, C.-C.; Lin, D.P.-C. Prevention of early Alzheimer's disease by erinacine A-enriched *Hericium erinaceus* mycelia pilot double-blind placebo-controlled study. *Front. Aging Neurosci.* **2020**, *12*, 155. [CrossRef]
20. Chiu, C.-H.; Chyau, C.-C.; Chen, C.-C.; Lee, L.-Y.; Chen, W.-P.; Liu, J.-L.; Lin, W.-H.; Mong, M.-C. Erinacine A-Enriched *Hericium erinaceus* Mycelium Produces Antidepressant-Like Effects through Modulating BDNF/PI3K/Akt/GSK-3β Signaling in Mice. *Int. J. Mol. Sci.* **2018**, *19*, 341. [CrossRef]
21. Kuo, H.; Lu, C.C.; Shen, C.H.; Tung, S.Y.; Hsieh, M.C.; Lee, K.C.; Lee, L.Y.; Chen, C.C.; Teng, C.C.; Huang, W.S.; et al. *Hericium erinaceus* mycelium and its isolated erinacine A protection from MPTP-induced neurotoxicity through the ER stress, triggering an apoptosis cascade. *J. Transl. Med.* **2016**, *14*, 78. [CrossRef]
22. Thongbai, B.; Rapior, S.; Hyde, K.D.; Wittstein, K.; Stadler, M. *Hericium erinaceus*, an amazing medicinal mushroom. *Mycol. Prog.* **2015**, *14*, 1–23. [CrossRef]
23. Zhang, C.-C.; Cao, C.-Y.; Kubo, M.; Harada, K.; Yan, X.-T.; Fukuyama, Y.; Gao, J.-M. Chemical Constituents from *Hericium erinaceus* Promote Neuronal Survival and Potentiate Neurite Outgrowth via the TrkA/Erk1/2 Pathway. *Int. J. Mol. Sci.* **2017**, *18*, 1659. [CrossRef] [PubMed]
24. Tsai-Teng, T.; Chin-Chu, C.; Li-Ya, L.; Wan-Ping, C.; Chung-Kuang, L.; Chien-Chang, S.; Chi-Ying, H.F.; Chien-Chih, C.; Shiao, Y.-J. Erinacine A-enriched *Hericium erinaceus* mycelium ameliorates Alzheimer's disease-related pathologies in APPswe/PS1dE9 transgenic mice. *J. Biomed. Sci.* **2016**, *23*, 49. [CrossRef] [PubMed]
25. Mori, K.; Inatomi, S.; Ouchi, K.; Azumi, Y.; Tuchida, T. Improving effects of the mushroom Yamabushitake (*Hericium erinaceus*) on mild cognitive impairment: A double-blind placebo-controlled clinical trial. *Phytother. Res.* **2009**, *23*, 367–372. [CrossRef]
26. Li, I.-C.; Lee, L.-Y.; Chen, Y.-J.; Chou, M.-Y.; Wang, M.-F.; Chen, W.-P.; Chen, Y.-P.; Chen, C.-C. Erinacine A-enriched *Hericium erinaceus* mycelia promotes longevity in Drosophila melanogaster and aged mice. *PLoS ONE* **2019**, *14*, e0217226. [CrossRef]
27. Azad, R.K.; Shulaev, V. Metabolomics technology and bioinformatics for precision medicine. *Brief Bioinform.* **2019**, *20*, 1957–1971. [CrossRef]
28. Zhou, Y.; Oh, M.H.; Kim, Y.J.; Kim, E.-y.; Kang, J.; Chung, S.; Ju, C.; Kim, W.-K.; Lee, K. Metabolism and Pharmacokinetics of SP-8356, a Novel (1S)-(−)-Verbenone Derivative, in Rats and Dogs and Its Implications in Humans. *Molecules* **2020**, *25*, 1775. [CrossRef]
29. Li, T.-J.; Lin, T.-W.; Wu, S.-P.; Chu, H.-T.; Kuo, Y.-H.; Chiou, J.-F.; Lu, L.-S.; Chen, C.-C. Patient-Derived Tumor Chemosensitization of GKB202, an Antrodia Cinnamomea Mycelium-Derived Bioactive Compound. *Molecules* **2021**, *26*, 6018. [CrossRef]
30. Shimbo, M.; Kawagishi, H.; Yokogoshi, H. Erinacine A increases catecholamine and nerve growth factor content in the central nervous system of rats. *Nutr. Res.* **2005**, *25*, 617–623. [CrossRef]
31. Li, I.C.; Chen, Y.L.; Lee, L.Y.; Chen, W.P.; Tsai, Y.T.; Chen, C.C.; Chen, C.S. Evaluation of the toxicological safety of erinacine A-enriched *Hericium erinaceus* in a 28-day oral feeding study in Sprague-Dawley rats. *Food Chem. Toxicol.* **2014**, *70*, 61–67. [CrossRef]
32. Tsai, P.C.; Wu, Y.K.; Hu, J.H.; Li, I.C.; Lin, T.W.; Chen, C.C.; Kuo, C.F. Preclinical Bioavailability, Tissue Distribution, and Protein Binding Studies of Erinacine A, a Bioactive Compound from *Hericium erinaceus* Mycelia Using Validated LC-MS/MS Method. *Molecules* **2021**, *26*, 4510. [CrossRef]
33. Pines, H.; Manassen, J. The Mechanism of Dehydration of Alcohols over Alumina Catalysts. *Adv. Catal.* **1966**, *16*, 49–93.
34. Bockisch, C.; Lorance, E.D.; Hartnett, H.E.; Shock, E.L.; Gould, I.R. Kinetics and Mechanisms of Dehydration of Secondary Alcohols Under Hydrothermal Conditions. *ACS Earth Space Chem.* **2018**, *2*, 821–832. [CrossRef]
35. Bhandari, D.R.; Shen, T.; Römpp, A.; Zorn, H.; Spengler, B. Analysis of cyathane-type diterpenoids from Cyathus striatus and *Hericium erinaceus* by high-resolution MALDI MS imaging. *Anal. Bioanal. Chem.* **2014**, *406*, 695–704. [CrossRef]
36. Farnberger, J.E.; Richter, N.; Hiebler, K.; Bierbaumer, S.; Pickl, M.; Skibar, W.; Zepeck, F.; Kroutil, W. Biocatalytic methylation and demethylation via a shuttle catalysis concept involving corrinoid proteins. *Commun. Chem.* **2018**, *1*, 1–8. [CrossRef]
37. Halpern, J. Mechanism and Stereoselectivity of Asymmetric Hydrogenation. *Science* **1982**, *217*, 401–407. [CrossRef]
38. SIEGEL, S. Alkene hydrogenation and related reactions A comparison of heterogeneous with homogeneous catalysis. *J. Catal.* **1973**, *30*, 139–145. [CrossRef]
39. Ortiz de Montellano, P.R. Hydrocarbon Hydroxylation by Cytochrome P450 Enzymes. *Chem. Rev.* **2010**, *110*, 932–948. [CrossRef]
40. Bond, G.C.; Wells, P.B. The Mechanism of the Hydrogenation of Unsaturated Hydrocarbons on Transition Metal Catalysts. *Adv. Catal.* **1965**, *15*, 91–226.
41. Diao, X.; Huestis, M.A. New Synthetic Cannabinoids Metabolism and Strategies to Best Identify Optimal Marker Metabolites. *Front. Chem.* **2019**, *7*, 109. [CrossRef]
42. Watanabe, S.; Kuzhiumparambil, U.; Nguyen, M.A.; Cameron, J.; Fu, S. Metabolic Profile of Synthetic Cannabinoids 5F-PB-22, PB-22, XLR-11 and UR-144 by Cunninghamella elegans. *AAPS J.* **2017**, *19*, 1148–1162. [CrossRef]
43. Ma, B.J.; Yu, H.Y.; Shen, J.W.; Ruan, Y.; Zhao, X.; Zhou, H.; Wu, T.T. Cytotoxic aromatic compounds from Hericium erinaceum. *J. Antibiot.* **2010**, *63*, 713–715. [CrossRef]

44. Kawagishi, H.; Ando, M.; Mizuno, T. Hericenone A and B as cytotoxic principles from the mushroom Hericium erinaceum. *Tetrahedron. Lett.* **1990**, *31*, 373–376. [CrossRef]
45. Yew Keong, C.; Amini Abdul Rashid, B.; Swee Ing, Y.; Ismail, Z. Quantification and identification of polysaccharide contents in *Hericium erinaceus*. *Nutr. Food Sci.* **2007**, *37*, 260–271. [CrossRef]
46. Abrams, M.E.; Johnson, K.A.; Perelman, S.S.; Zhang, L.S.; Endapally, S.; Mar, K.B.; Thompson, B.M.; McDonald, J.G.; Schoggins, J.W.; Radhakrishnan, A. Oxysterols provide innate immunity to bacterial infection by mobilizing cell surface accessible cholesterol. *Nat. Microbiol.* **2020**, *5*, 929–942. [CrossRef]